Pattern Competition in Temporally Modulated Rayleigh-Bénard Convection

Christopher W. Meyer,[1] David S. Cannell,[1] Guenter Ahlers,[1] J. B. Swift,[2] and P. C. Hohenberg[3]
[1]*Department of Physics, University of California, Santa Barbara, Santa Barbara, California 93106*
[2]*Department of Physics and Center for Nonlinear Dynamics, University of Texas, Austin, Texas 78712*
[3]*AT&T Bell Laboratories, Murray Hill, New Jersey 07974*
(Received 31 May 1988)

Shadowgraph flow-visualization studies and heat-flux measurements were used to study convection subjected to temporal modulation of the Rayleigh number R in the form $\epsilon(t)=R(t)/R_c^{\rm stat}-1=\epsilon_0+\delta\sin(\omega t)$, where $R_c^{\rm stat}$ is the unmodulated threshold, and ω and t are scaled by the vertical thermal diffusion time. For $\omega=15$ and $0.7\lesssim\delta\lesssim 2.0$ the predicted hexagonal patterns were observed for a range of ϵ_0 immediately above the convective threshold ϵ_c. With increasing ϵ_0 there is a region exhibiting coexistence between hexagons and rolls, followed by roll-like patterns. The observed boundaries between these regions and the magnitude of the convective heat transport are consistent with theory.

PACS numbers: 47.20.Bp, 47.20.Ky, 47.25.Qv

The problem of Rayleigh-Bénard convection subjected to external temporal modulation of the Rayleigh number R has been studied both theoretically and experimentally.[1-8] The emphasis of that work has been primarily on the shift of the critical Rayleigh number R_c for the onset of convection.[1,2,4] This shift can be obtained from the *linearized* equations of motion. Its predicted value $R_c(\delta,\omega)-R_c^{\rm stat}$ depends upon the modulation amplitude δ and frequency ω, and was recently confirmed in experimental work by Niemela and Donnelly.[8] Theoretical attention has also been devoted to the nature of the bifurcation at R_c and to the convective pattern above onset.[3,6] These are *nonlinear* aspects of the problem. For convection in a fluid which satisfies the Oberbeck-Boussinesq (OB) approximation, it is known[9] that the bifurcation at R_c is supercritical and that the pattern immediately above onset in a laterally infinite layer consists of straight, parallel rolls when R is held constant. In a non-OB system, where one or more fluid properties are significantly temperature dependent, the bifurcation is subcritical and a hexagonal pattern is stable immediately above onset.[10-12] A hexagonal pattern can also be stabilized in an OB fluid by subjecting the system to a time-dependent top and/or bottom temperature.[3,6,13] In that case the nonlinear temperature profile of the conduction state plays much the same role as the temperature variation of the fluid properties in the non-OB case in that it breaks the symmetry between the regions of upflow and downflow. Krishnamurti[13] has shown theoretically and experimentally that hexagons can be generated by steadily increasing or decreasing the top and bottom temperatures simultaneously as functions of time. Roppo, Davis, and Rosenblat[3] (RDR) have predicted theoretically that these effects can be created by external temporal modulation of the temperature difference across the fluid layer. This case has the advantage that it permits the experimental investigation of a stationary state. The theory of RDR involved a perturbation expansion in the amplitude δ, whose validity was shown[6] to be limited to the range $\delta/\omega\approx 0.06$. Recently, two of us (P.C.H. and J.B.S., hereafter referred to as HS), derived a thirteen-mode Lorenz model,[6] whose solution confirmed the qualitative prediction of RDR, but which was not limited to small values of δ, where the stability range of hexagons is unobservably small.[6] An important conclusion of HS was that there is an optimal frequency range for observing hexagons, since their stability region vanishes not only for $\omega\to\infty$, but also for $\omega\to 0$. It is the absence of this feature which makes the results of perturbation theory[3] qualitatively incorrect at low frequency.

In this Letter we report on experimental observations of hexagons in Rayleigh-Bénard convection subjected to external temporal modulation. We observed regions in parameter space exhibiting pure hexagonal patterns and pure roll patterns. Their boundaries are consistent with those predicted by HS. However, in the region where the model predicts bistability and hysteresis we observed a nonhysteretic coexistence between hexagons and rolls.

A special apparatus for achieving large-amplitude modulations was built. The working fluid was water near 51°C, with a Prandtl number equal to 3.6. We used an acrylic sidewall with height $d=0.350$ cm and an inner diameter of 7.70 cm. The top plate of the cell was made of sapphire and held at 50.6°C by a temperature-controlled bath. The bottom plate was made of copper with polished nickel on its upper surface, for use with the shadowgraph flow-visualization technique.[14] A heater was embedded in the bottom of the copper plate. A 0.05-cm-thick acrylic plate was epoxied to the bottom of this plate, providing a thermal resistance between it and a heat-sinking bath in contact with the lower surface of the acrylic. This bath was maintained at 14.3°C, and both baths were held constant to within 0.002°C. By applying a large heat current to the bottom plate, we could raise the temperature of the plate to its desired

© 1988 The American Physical Society

mean temperature. Then, by our modulating the heat current about its mean value, substantial modulation of the temperature of the bottom plate could be achieved. The range $\omega\delta \lesssim 30$ can be explored with this design.

The experiment involved our modulating the heat current sinusoidally, resulting in

$$\epsilon(t) \equiv \frac{R(t)}{R_c^{\text{stat}}} - 1$$

$$= \epsilon_0 + \delta \sin(\omega\delta) + (\text{higher harmonics}),$$

where $R(t)$ is the instantaneous Rayleigh number[4] based on the temperature difference $\Delta T(t)$, and R_c^{stat} is the unmodulated convective threshold. The frequency ω and the time t are scaled[4] by the vertical thermal diffusion time d^2/κ, where κ is the thermal diffusivity of the fluid. Here we report on results for $\omega = 15$, a frequency that was sufficiently low that hexagons are predicted[6] to be observable and sufficiently high that the stochastically induced, irreproducible patterns seen under low-frequency modulation[7] do not occur.

The theoretical bifurcation diagram[3,6,10] relating to hexagon-roll stability near onset in a laterally infinite system is shown schematically in the inset of Fig. 1. A positive threshold shift changes the convective onset from $\epsilon_0 = 0$ to $\epsilon_0 = \epsilon_c$. Immediately above ϵ_c, roll patterns, which appear through a supercritical bifurcation, are unstable to hexagonal patterns. This continues as ϵ_0 is increased until $\epsilon_0 = \epsilon_R$, beyond which rolls are stable. The hexagons appear through a subcritical bifurcation, first becoming stable at $\epsilon_0 = \epsilon_A < \epsilon_c$ and continuing to be stable until $\epsilon_0 = \epsilon_B > \epsilon_R$, where they become unstable to rolls. For $\epsilon_R \leq \epsilon_0 < \epsilon_B$ both hexagons and rolls are linearly stable. While this bistable region is large and observable, the region $\epsilon_A \leq \epsilon_0 < \epsilon_c$ is predicted to be small,[6] and we were not able to detect it. The thresholds ϵ_c, ϵ_R, and ϵ_B predicted by HS for $\omega = 15$ are shown as functions of δ in Fig. 1 as solid lines.

During the course of each modulation cycle, the pattern became visible and then faded from view. After a sufficient number of cycles, the patterns which appeared in successive cycles became indistinguishable. Figure 2(a) is a shadowgraph image of the central portion of

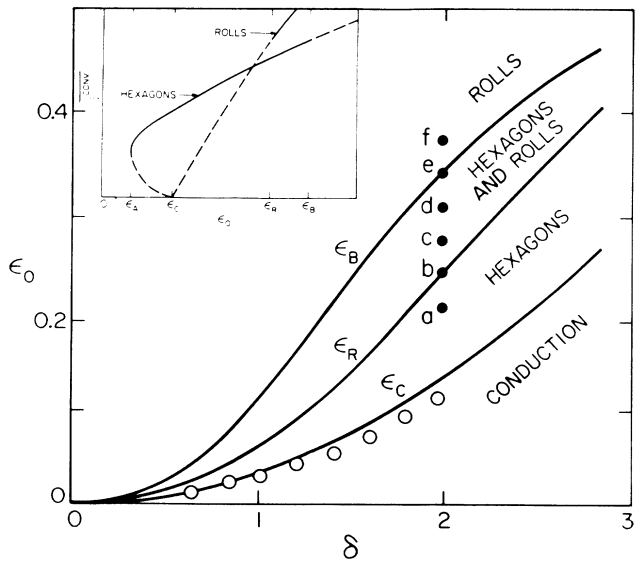

FIG. 1. Stability limits in the ϵ_0-δ plane for modulated convection with $\omega = 15$. The solid curves show the predictions (see Ref. 6) of the Lorenz model for ϵ_c, ϵ_R, and ϵ_B. The open circles are our experimental measurements (see Ref. 15) of ϵ_c, while the solid circles show the locations of the images in Fig. 4. Inset: Theoretical bifurcation diagram showing schematically the convective current averaged over a cycle, $\bar{j}^{\text{conv}}$, as a function of the mean of the reduced Rayleigh number ϵ_0. The dashed lines represent unstable solutions. Modulation shifts the convective threshold from $\epsilon_0 = 0$ to $\epsilon_0 = \epsilon_c$. Hexagonal flow occurs through a subcritical bifurcation and is stable for $\epsilon_A \leq \epsilon_0 < \epsilon_B$. The bifurcation to rolls is supercritical, but rolls are stable only above ϵ_R. Note that the definitions of ϵ_A, ϵ_R, and ϵ_B used here differ from those of Ref. 6 by the overall additive constant ϵ_c.

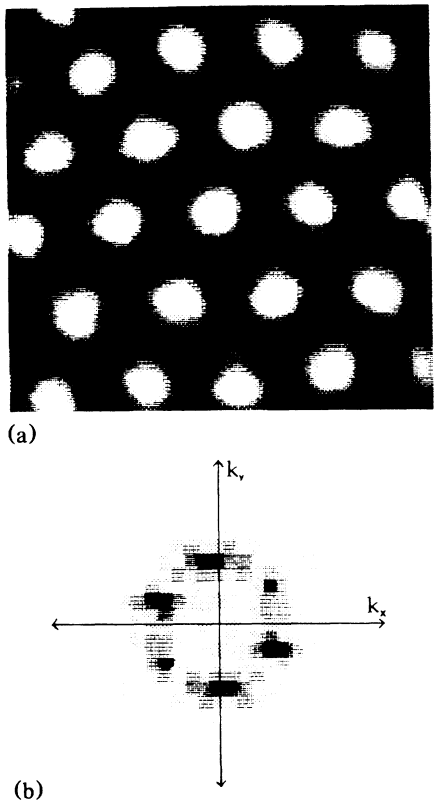

FIG. 2. (a) Shadowgraph image of a hexagonal convection pattern achieved with modulation parameters $\omega = 15$, $\delta = 1.97$, and $\epsilon_0 = 0.20$. The bright regions show downflow at the center of the hexagons, while the dark regions show upflow along their outer boundaries. (b) Low-wave-vector portion of the Fourier transform of the image in (a), demonstrating the sixfold symmetry of the pattern.

such a steady-state pattern under conditions where hexagons are stable ($\omega=15$, $\delta=1.97$, $\epsilon_0=0.20$). This image was taken close to the time when the pattern intensity reached its peak. The bright regions show downflow in the center of the hexagons, and the dark regions show upflow along their outer boundaries, confirming the direction of flow within the hexagons predicted by theory.[3] Figure 2(b) displays the low-wave-vector portion of the Fourier transform of the image, clearly demonstrating the sixfold symmetry of the pattern.

We determined ϵ_c from heat-flux measurements, examples of which are shown in Fig. 3. The average over one cycle of the part of the heat current attributable to convection, $\bar{j}^{\rm conv}$, is plotted as a function of ϵ_0 ($j^{\rm conv}$ is scaled by the critical heat current for the onset of unmodulated convection). Static heat-flux measurements are shown as open circles, and the solid line through the points is the prediction of the model for $\delta=0$, with a small adjustment of the slope[4] to account for the finite geometry. Points from measurements taken under modulation with $\omega=15$ and $\delta=1.97$ are plotted as solid circles. The threshold was determined by our fitting a line through the points where, within our resolution, $\bar{j}^{\rm conv}$ appears to increase linearly with ϵ_0 and then extrapolating this line to the point[15] where $\bar{j}^{\rm conv}=0$. Measurements of ϵ_c for other values of δ are shown as open circles in Fig. 1. They are seen to be consistent with the model within our possible systematic errors.[15]

In order to explore the stability limits of the hexagons and rolls, we performed an experiment in which we started with $\epsilon_0=-0.2$ and incremented ϵ_0 in steps of approximately 0.02. For each value of ϵ_0 we modulated with $\omega=15$ and $\delta=1.97$ for forty cycles, a number adequate to achieve a steady state. In the fortieth cycle we took an image of the pattern at its peak intensity in the cycle. At the end of this cycle we immediately increased ϵ_0 and resumed the modulation without loss of temporal coherence with the previous cycles. The heat-flux measurements plotted in Fig. 3 were obtained from this experiment, and the solid lines are the predictions of HS with the results for both hexagons and rolls shown whenever they are stable. The theoretical curve, which has no adjustable parameters, is seen to agree well with the data in the pure hexagon ($\epsilon_c \le \epsilon_0 < \epsilon_R$) and pure roll ($\epsilon_0 > \epsilon_B$) regions. In the bistable region ($\epsilon_R \le \epsilon_0 < \epsilon_B$) the model predicts either hexagons or rolls, depending on initial conditions, but not both. However, the experimental heat-flux data do not reveal this hysteresis loop.

The actual patterns observed can be seen from the images in Fig. 4, which correspond to parameter values shown as solid circles in Fig. 1. Pattern 4(a), taken in this region where only hexagons are predicted to be stable, is essentially hexagonal with some defects and

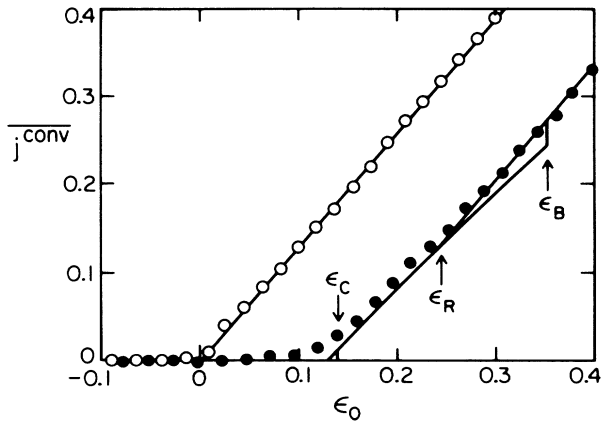

FIG. 3. The convective heat current averaged over one cycle vs ϵ_0. The open circles are from static measurements ($\delta=0$). The solid circles show the measurements from a modulation experiment with $\omega=15$ and $\delta=1.97$. The solid curves are the prediction of the Lorenz model (see Ref. 6). Only stable states are shown. Note the small hysteretic loop immediately below ϵ_c.

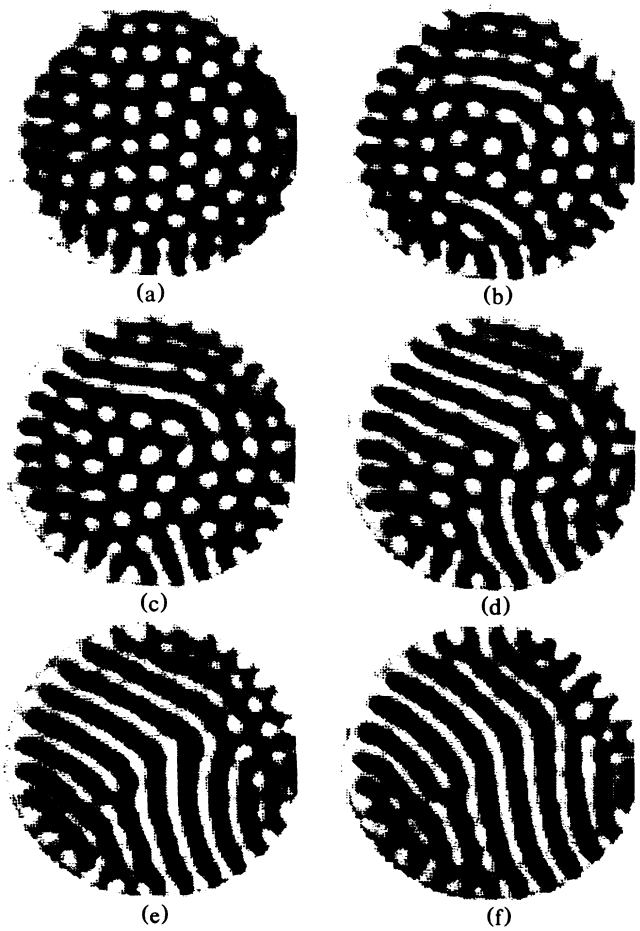

FIG. 4. Images of convective flow patterns for $\omega=15$, $\delta=1.97$, and (a) $\epsilon_0=0.21$, (b) 0.25, (c) 0.29, (d) 0.32, (e) 0.36, and (f) 0.40.

distortions which we believe to be due to the geometrical constraint of circular sidewalls. Pattern 4(f) is the corresponding one for rolls, whereas patterns 4(b)–4(e) show clear signs of *spatial coexistence* of hexagons and rolls.[16] The corresponding heat-flow measurements are shown in Fig. 3. They fall on a smooth curve connecting the value of $\bar{j}^{\mathrm{conv}}$ at ϵ_R to that at ϵ_B. This behavior contrasts with that found in previous work on non-OB convection,[12] where the hysteresis loops between ϵ_R and ϵ_B, as well as between ϵ_A and ϵ_c, were clearly observable in heat-flux measurements. Since the Lorenz model developed by HS does not allow for spatial variations, it is inadequate for studying the coexistence of hexagon and roll patterns, and further work is required to address these interesting questions.

In summary, we have presented quantitative data showing that temporal modulation allows one to control the pattern of convection near onset over a substantial experimental range. The phenomena can be analyzed with use of a simple model obtained from hydrodynamic equations with no adjustable parameters.

The work of the University of California, Santa Barbara, group was supported by U.S. Department of Energy Grant No. DE-FG03-87ER13738. One of us (J.B.S.) was supported by the R. A. Welch Foundation under Grant No. F-767 and U.S. Department of Energy Grant No. DE-AS05-84ER13147.

[1]For a review of early work, see S. H. Davis, Annu. Rev. Fluid Mech. **8**, 57 (1976).

[2]S. Rosenblat and G. A. Tanaka, Phys. Fluids **14**, 1319 (1971).

[3]M. N. Roppo, S. H. Davis, and S. Rosenblat, Phys. Fluids **27**, 796 (1984).

[4]G. Ahlers, P. C. Hohenberg, and M. Lücke, Phys. Rev. A **32**, 3493, 3519 (1985).

[5]J. J. Niemela and R. J. Donnelly, Phys. Rev. Lett. **57**, 583 (1986).

[6]P. C. Hohenberg and J. B. Swift, Phys. Rev. A **35**, 3855 (1987). The thirteen modes are x_{nj}, y_{nj} and $z(n=1,2; j=1,2,3)$ of Eqs. (2.6) of HS. The equations of motion are obtained from Eq. (2.7) by permutation on the index j.

[7]C. W. Meyer, G. Ahlers, and D. S. Cannell, Phys. Rev. Lett. **59**, 1577 (1987).

[8]J. J. Niemela and R. J. Donnelly, Phys. Rev. Lett. **59**, 2431 (1987).

[9]A. Schlüter, D. Lortz, and F. H. Busse, J. Fluid Mech. **23**, 129 (1965).

[10]See F. H. Busse, J. Fluid Mech. **30**, 625 (1967), and references therein.

[11]M. Dubois, P. Bergé, and J. Wesfreid, J. Phys. (Paris) **39**, 1253 (1978).

[12]R. W. Walden and G. Ahlers, J. Fluid Mech. **109**, 89 (1981).

[13]R. Krishnamurti, J. Fluid Mech. **33**, 445, 457 (1968).

[14]V. Steinberg, G. Ahlers, and D. S. Cannell, Phys. Scr. **32**, 534 (1985).

[15]Because of the small, but noticeable rounding of the convective onset, as well as because of the subcritical nature of the bifurcation to hexagons, this procedure will tend to underestimate ϵ_c by a small amount. We have not determined the size of this systematic error. Note that the line in Fig. 3 is the theoretical prediction of HS, not the line used to determine ϵ_c.

[16]After modulation for up to 200 cycles the coexistence remained. Furthermore, runs starting with pure hexagons or with pure rolls as initial patterns yielded qualitatively similar coexistence after 200 cycles.

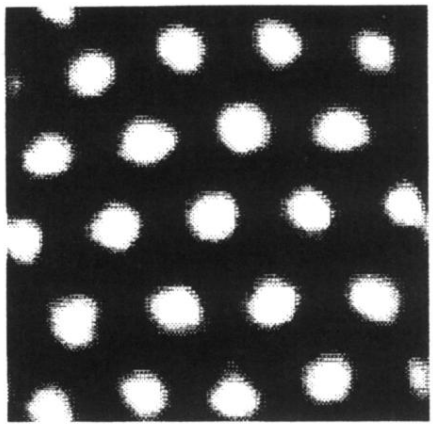

(a)

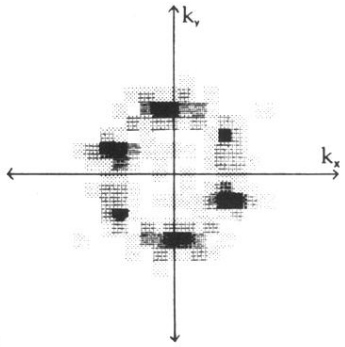

(b)

FIG. 2. (a) Shadowgraph image of a hexagonal convection pattern achieved with modulation parameters $\omega=15$, $\delta=1.97$, and $\epsilon_0=0.20$. The bright regions show downflow at the center of the hexagons, while the dark regions show upflow along their outer boundaries. (b) Low-wave-vector portion of the Fourier transform of the image in (a), demonstrating the sixfold symmetry of the pattern.

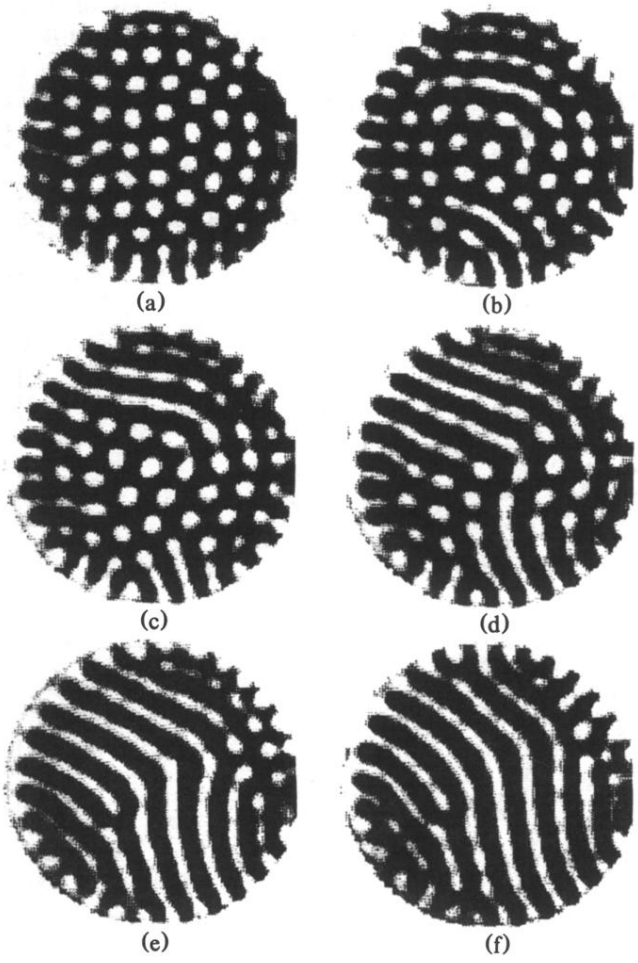

FIG. 4. Images of convective flow patterns for $\omega = 15$, $\delta = 1.97$, and (a) $\epsilon_0 = 0.21$, (b) 0.25, (c) 0.29, (d) 0.32, (e) 0.36, and (f) 0.40.